ACCOUNTS
of chemical research

Designing Dipolar Recoupling and Decoupling Experiments for Biological Solid-State NMR Using Interleaved Continuous Wave and rf Pulse Irradiation

MORTEN BJERRING, SHEETAL JAIN, BERIT PAASKE,
JOACHIM M. VINTHER, AND NIELS CHR. NIELSEN*

Center for Insoluble Protein Structures (inSPIN), Interdisciplinary Nanoscience Center (iNANO) and Department of Chemistry, Aarhus University, Denmark

CONSPECTUS

Rapid developments in solid-state NMR methodology have boosted this technique into a highly versatile tool for structural biology. The invention of increasingly advanced rf pulse sequences that take advantage of better hardware and sample preparation have played an important part in these advances. In the development of these new pulse sequences, researchers have taken advantage of analytical tools, such as average Hamiltonian theory or lately numerical methods based on optimal control theory.

In this Account, we focus on the interplay between these strategies in the systematic development of simple pulse sequences that combines continuous wave (CW) irradiation with short pulses to obtain improved rf pulse, recoupling, sampling, and decoupling performance. Our initial work on this problem focused on the challenges associated with the increasing use of fully or partly deuterated proteins to obtain high-resolution, liquid-state-like solid-state NMR spectra. Here we exploit the overwhelming presence of ^{2}H in such samples as a source of polarization and to gain structural information. The ^{2}H nuclei possess dominant quadrupolar couplings which complicate even the simplest operations, such as rf pulses and polarization transfer to surrounding nuclei. Using optimal control and easy analytical adaptations, we demonstrate that a series of rotor synchronized short pulses may form the basis for essentially ideal rf pulse performance.

Using similar approaches, we design ^{2}H to ^{13}C polarization transfer experiments that increase the efficiency by one order of magnitude over standard cross polarization experiments. We demonstrate how we can translate advanced optimal control waveforms into simple interleaved CW and rf pulse methods that form a new cross polarization experiment. This experiment significantly improves ^{1}H$-^{15}$N and ^{15}N$-^{13}$C transfers, which are key elements in the vast majority of biological solid-state NMR experiments. In addition, we demonstrate how interleaved sampling of spectra exploiting polarization from ^{1}H and ^{2}H nuclei can substantially enhance the sensitivity of such experiments. Finally, we present systematic development of ^{1}H decoupling methods where CW irradiation of moderate amplitude is interleaved with strong rotor-synchronized refocusing pulses. We show that these sequences remove residual cross terms between dipolar coupling and chemical shielding anisotropy more effectively and improve the spectral resolution over that observed in current state-of-the-art methods.
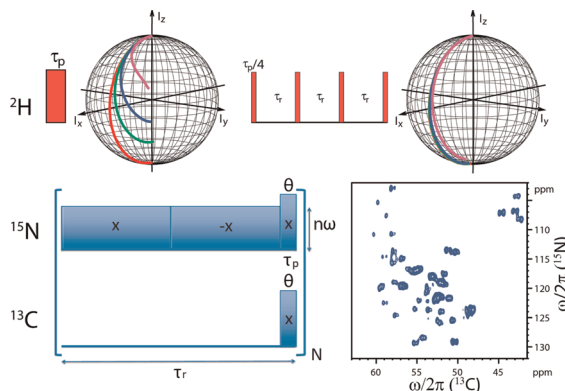
Introduction

Solid-state NMR has undergone an impressive development to become a tool used in wide areas of research ranging from materials science to structural biology. This has been driven by advances in hardware, sample preparation, pulse methods, and data interpretation software.

Hardware improvements involve, for example, stronger magnets, faster rf, hyperpolarization, and probes with fast magic-angle spinning[1] (MAS). For biological applications, large-scale sample preparation methods have been established to generate homogeneous samples with uniform, sparse, or specific incorporation of ^{13}C, ^{15}N, or ^{2}H isotopes.[2-5]

In parallel, there has been extensive development of pulse sequences and software facilitating studies of structure and dynamics of increasingly complex biological systems.[6,7]

NMR is an insensitive technique, which for solids faces problems with broad lines and low spectral resolution. In absence of fast isotropic molecular motion, anisotropic nuclear spin interactions lead to severe line broadening. The dominant part of this broadening may be eliminated using oriented samples,[8] as used to study proteins in lipid bilayers[9−13] (review in ref 14) or MAS with the sample rotating fast around an axis inclined by 54.74° with respect to the static field. In this manner, high-resolution spectra may be obtained routinely for, e.g., ^{13}C and ^{15}N. To improve the resolution and establish spin connectivities, it is commonplace to spread the signals into multidimensional spectra. Such methods are now highly developed and numerous structural studies have been carried out on proteins in microcrystalline[4,15−19] and fibrillar[20−24] form as well as on membrane proteins in lipid environments[25−27] and proteins in larger complexes.[28,29]

Multidimensional MAS NMR relies on magnetization transfer between various nuclei, for example, ^{1}H→^{13}C, ^{13}C→^{13}C, or ^{15}N→^{13}C. These transfers rely on reintroduction (so-called *recoupling*) of the relevant dipole−dipole couplings which in MAS experiments are averaged by sample spinning. Since sensitivity is a crucial issue, large efforts are put into optimizing the efficiencies of such elements. The need for efficient transfers can be rationalized by a multidimensional experiment, typically involving 2−4 recoupling elements. An efficiency of 40% in each transfer has as consequence that only 3−16% of the magnetization "survives" the transfers, whereas an efficiency of 66% leaves 20−44% for acquisition. The implication is that to obtain the same signal-to-noise ratio in the spectra after two-four recoupling elements for the two cases, the time needed for the "low efficiency case" can be 8−40 times that of the latter, strongly motivating development of efficient recoupling methods to retain *sensitivity*.

With similar aim, it is of interest to exploit all resources of polarization, that is, focusing on nuclei with high gyromagnetic ratio and abundance. Here excitation/detection through ^{1}H spins is obvious, as used extensively in liquid-state NMR. In solid-state NMR, there is an increasing interest in ^{1}H detection, being complicated by strong ^{1}H−^{1}H dipolar couplings calling for homonuclear decoupling, extremely fast spinning, and so forth. An alternative approach involves dilution of ^{1}H spins (e.g., 5−10% protons at labile sites; corresponding to 1−2% of the proton sites) through extensive deuteration during preparation.[30−37] This leads to a gain in sensitivity through detection of ^{1}H, but also substantial loss in sensitivity due to dilution of the detectable spins. Thus, it may be of interest also to look into the deuteron polarization.

In addition to sensitivity, it is crucial to obtain optimum spectral *resolution* calling for efficient heteronuclear decoupling methods removing residual couplings between the detected spins and surrounding hetero nuclei. The most commonplace situation is ^{13}C detection in samples with abundant ^{1}H spins, which calls for efficient ^{1}H decoupling. This challenge has motivated design of increasingly advanced decoupling experiments.

Addressing the needs for *sensitivity and resolution* in biological solid-state NMR, we will in this Account demonstrate systematic development of efficient rf pulses, dipolar recoupling, interleaved sampling, and heteronuclear decoupling methods eventually represented as simple combinations of continuous wave (CW) irradiation and interleaving rf pulses.

Efficient rf Manipulation of ^{2}H Spins

Dilution of protons by ^{2}H paves the way for ^{1}H-detected solid-state NMR. Relating to proteins, this may be accomplished through expression of perdeuterated samples combined with reintroduction of ^{1}H at labile positions. Such preparations have proven useful to obtain highly resolved ^{1}H-detected spectra.[30−37] The use of deuterated samples renders it relevant to exploit the abundant deuterons, not only as a source of sensitivity but also as probes for dynamics[38] or separating domains capable of or not capable of ^{1}H exchange. For this to be realized, it is fundamental to have efficient rf pulses for ^{2}H. The complication herein is the presence of a quadrupolar coupling interaction, in the order of 200 kHz in frequency units. This markedly influences the effect of rf pulses unless very strong rf fields are applied, as illustrated in Figure 1 showing single-pulse (Figure 1a) excitation and inversion of ^{2}H signals from U−^{2}H,^{13}C glutamine (Figure 1d). It is evident that inversion is inefficient and cannot be carried out using a simple single pulse at normal rf power. This is illustrated numerically in Figure 1f, where an extreme of 500 kHz rf irradiation is required for full inversion.

To develop pulse schemes, for example, addressing a challenge like efficient rf pulses for ^{2}H MAS NMR, typically analytical tools as average Hamiltonian theory (AHT),[39] refined AHT variants,[40,41] Floquet theory,[42] or numerical approaches have been employed. Recently, attention has devoted to numerical procedures relying on optimum control (OC) theory[43] where NMR-adapted algorithms[44−48] have proven useful for design of experiments in liquid-[49] and solid-state NMR,[50,51] as well as MRI.[52,53] The advantage
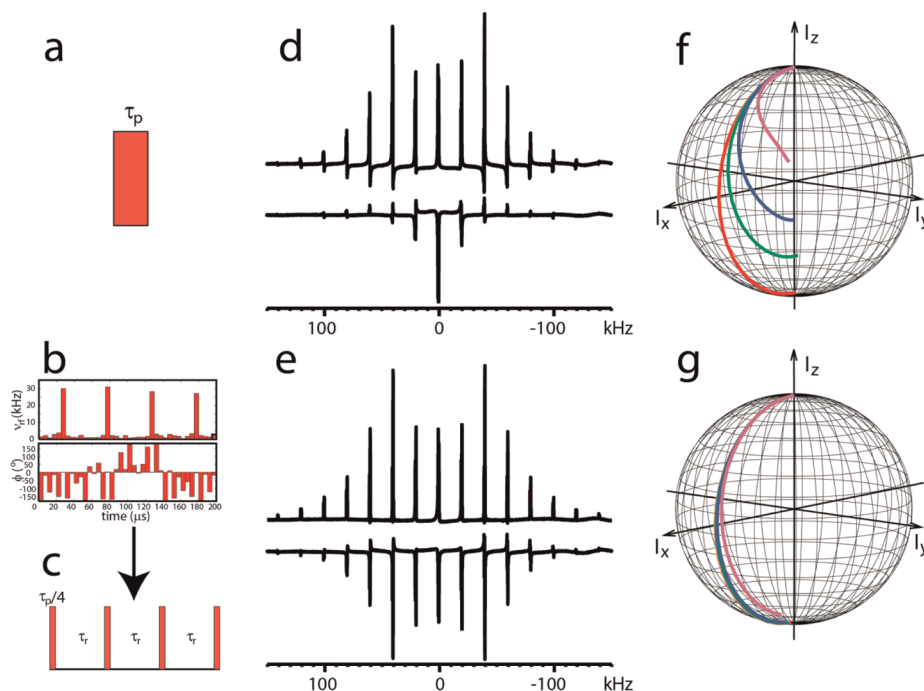
FIGURE 1. (a) ^{2}H rf pulse leading to the experimental excitation (upper) and inversion (lower) spectra of ^{2}H,^{13}C-glutamine in (d) using 50 kHz rf amplitude at 20 kHz MAS and to the simulated trajectories in (f) starting from I_z for a powder of ^{2}H spins (C_Q = 180 kHz, η = 0.1) using amplitudes of 500 (red), 100 (green), 60 (blue), and 30 (magenta) kHz. (b) Optimal control pulse (top, amplitude; bottom, phase), and (c) analytical RESPIRATION-4 pulse inspired from OC. (e) Experimental excitation (upper) and inversion (lower) spectra as in (d) acquired with the RESPIRATION-4 pulse. (g) Same trajectories as in (f) with the RESPIRATION-4 pulse. Figure reproduced with permission from ref 54. Copyright 2011 American Chemical Society.

of OC is that it enables consideration of all relevant parameters (related to instrument or spin system), and relative to standard nonlinear optimization it facilitates optimizations of a very large number of pulse variables. Accordingly, OC sequences take the form of arrays of pulses with varying amplitudes and phases, that is, rf waveforms.

Returning to pulses for ^{2}H MAS NMR, we applied OC in the design through specification of a powder of ^{2}H nuclei with typical quadrupolar coupling parameters, 400 MHz static field, 20 kHz MAS, a realistic limit for the rf field strength, as well as typical variations in offset and rf inhomogeneity. In the iterative optimization, the amplitudes and phases of 40 pulses of 5 μs each were varied to provide the inversion pulse in Figure 1b. Effectively, this pulse sequence consists of four pulses each separated by a rotor period among much weaker pulses. This simple OC sequence inspired a solution to ^{2}H pulses in MAS NMR, namely, so-called Rotor Echo Short Pulse IRrAdiaTION (RESPIRATION) pulses as shown in Figure 1c.[54] Such pulses are easy to understand in the sense that instead of a "long" pulse through which the orientation-dependent quadrupolar coupling varies and thereby induces different effects for different crystallites, the pulse is divided into small segments applied at the rotor echoes with identical influence from the anisotropic interaction each

time. It is seen from experimental spectra (Figure 1e) and simulations (Figure 1g) that the simple excitation scheme in Figure 1c is indeed useful. The RESPIRATION pulses, which can consist of two or more pulses each separated by a rotor period, may replace single pulses in experiments applied to quadrupolar nuclei where irregular pulse performance is a challenge. An independent study focusing on excitation of ^{14}N nuclei makes use of similar principles.[55]

Exploiting ^{2}H Polarization in Perdeuterated Proteins

Being able to control ^{2}H pulses, the next need is transfer of polarization from ^{2}H to nuclei such as ^{13}C and ^{15}N. Here the cross-polarization (CP) technique[56] does not perform adequately unless using very strong rf fields. This is not satisfactory, considering the desired use of ^{13}C and ^{15}N coherence for assignment and structural constraints. The typical arguments for CP is to exploit an advantage in polarization due to the higher gyromagnetic ratio of the donating spin, and also a gain in accumulation speed due to shorter T_1 of, for example, ^{1}H relative to ^{13}C.[56] In the former regard, the idea of transferring magnetization from ^{2}H to ^{13}C may seem counterintuitive considering that γ for ^{2}H is lower than for ^{13}C. However, T_1 is typical orders of magnitude shorter for ^{2}H
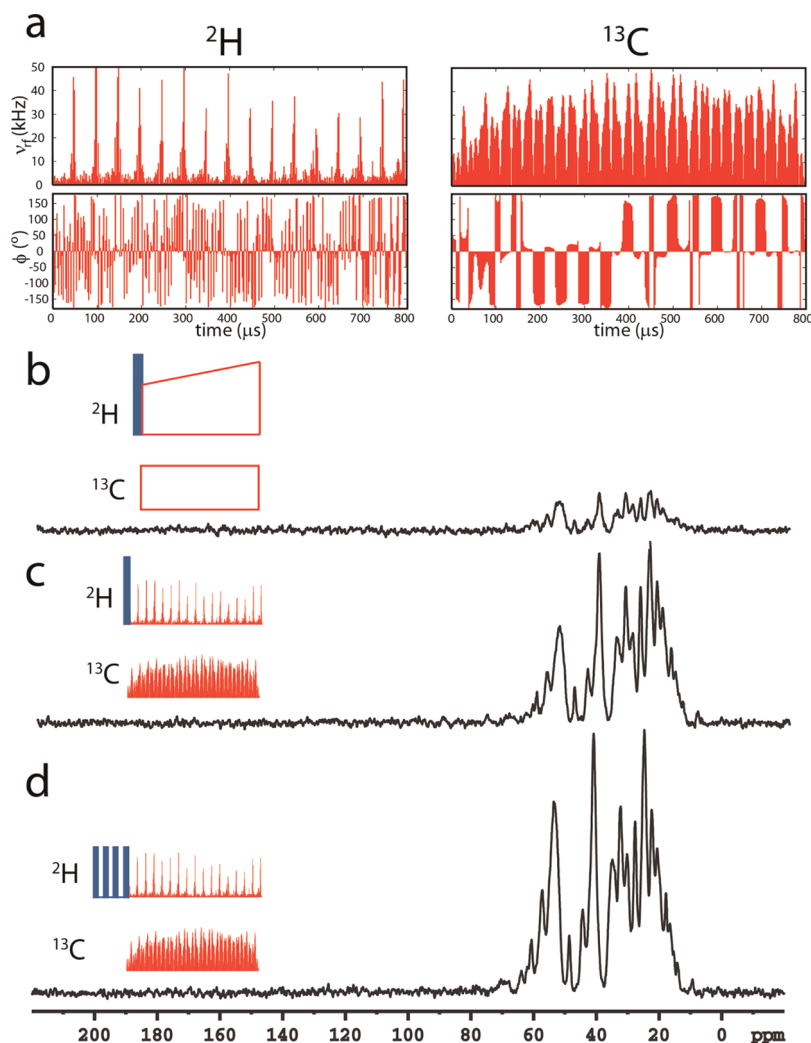
FIGURE 2. (a) rf amplitudes (top) and phases (bottom) for the ^{2}H (left) and ^{13}C (right) channels of an optimal control ^{2}H→^{13}C CP experiment. (b−d) ^{2}H→^{13}C transfer experiments (20 kHz spinning) of perdeuterated, amide ^{1}H back-exchanged U−^{13}C,^{15}N α spectrin SH$_3$ domain acquired using (b) ramped CP, (c) ^{OC}CP, and (d) RESPIRATION-4 ^{OC}CP. Figure reproduced with permission from ref 54. Copyright 2011 American Chemical Society.

than for ^{1}H and ^{13}C, paving the way for very fast experiment repetition when ^{2}H is taken as source. We note that with an extensively deuterated sample, high-power ^{1}H decoupling is not needed during acquisition. Another argument is the high abundance of ^{2}H relative to ^{1}H in deuterated samples, implying that the deuterons upon appropriate CP could contribute more ^{13}C or ^{15}N polarization than the ^{1}H spins.

Accordingly, it makes sense to develop the potential for ^{2}H→^{13}C transfer in perdeuterated samples. It is easily deduced that the simple CP experiment and e.g. ramped variants,[57] does not offer high efficiency and in simulations for a two-spin ^{2}H−^{13}C model, only 1/4−1/3 of the magnetization is transferred even using strong rf fields. Adapting the OC design strategy, it proves possible, even when including offsets and rf inhomogeneity, to achieve 85% efficiency.[54] phases and amplitudes for the OC pulse trains

(^{OC}CP) are shown in Figure 2a, and although looking chaotic, some systematics are visible, for example, for the ^{2}H rf amplitudes where strong pulses are separated by rotor periods.

An experimental demonstration of ^{2}H→^{13}C ^{OC}CP is given in Figure 2b−d for uniformly ^{2}H,^{13}C,^{15}N-labelled α spectrin SH3 with 100% ^{1}H back substitution at exchangeable sites. An optimized ramped CP spectrum is shown in Figure 2b, while Figure 2c provides the corresponding ^{OC}CP spectrum increasing the sensitivity by a factor of 4. Combining ^{OC}CP with initial RESPIRATION excitation (Figure 2d) adds another factor of 2.5, hereby approaching a factor of 10 relative to standard CP. The increase in sensitivity obtained replacing a standard 90° pulse with a RESPIRATION-4 90° pulse is ascribed to removal of the orientation dependent intensity and phase distortion produced by the conventional pulse (compare Figure 1f and g). Overall this demonstrates not

only the power of OC experiment design, but also provides us with two important elements (rf pulses and cross polarization) needed to exploit ^{2}H polarization in perdeuterated proteins.

Harvesting ^{1}H and ^{2}H Polarization through Interleaved Sampling

The strong interest in deuterated ^{13}C,^{15}N-labeled proteins with full/partial ^{1}H back substitution of the labile sites motivates design of experiments exploiting both ^{2}H and ^{1}H. As demonstrated above ^{2}H→^{13}C transfer serves as an efficient means for excitation of ^{13}C. However, as also revealed from Figure 2, for example, carbonyls are not excited in ^{2}H-based spectra since ^{2}H−^{13}C dipolar couplings are rather weak, and mostly transfer from ^{2}H to directly bonded ^{13}C is facilitated. Also, with ^{1}H back substitution, ^{1}H→^{13}C transfer remains attractive for ^{13}C excitation.

To exploit complementary ^{1}H→^{13}C and ^{2}H→^{13}C transfers, a sampling strategy using dual acquisition with a single receiver was developed which also pinpoints the inefficient use of spectrometers in standard experiments. In ^{13}C CP/MAS experiments, the time spent on the pulse sequence and acquisition typically last less than 50 ms whereas the repetition delay amounts to 2−4 s. One approach to more efficient spectrometer usage has been the introduction of paramagnetic agents in the sample which greatly reduce the ^{1}H T_1 relaxation time.[58−61] Another approach was based on different ^{13}C relaxation times and selective pulses.[62] Here we exploit the different relaxation times of ^{2}H and ^{1}H in partly deuterated proteins, with the specific T_1's depending on the degree of deuteration.[36] The much shorter T_1 for ^{2}H relative to ^{1}H makes it attractive to interleave ^{1}H- and ^{2}H-based experiments using the pulse sequence in Figure 3a. In this 1D version of the so-called Relaxation-optimized Acquisition of Protons Interleaved with Deuterium (RAPID) experiment,[36] 8−16 ^{2}H→^{13}C RESPIRATION ^{OC}CP scans are recorded for each ^{1}H→^{13}C CP scan. Hereby the waiting time for the proton experiment is used to take complementary polarization from the deuterons. Figure 3e demonstrates the possibility to enhance the overall sensitivity through summation of simultaneously sampled spectra from ^{1}H→^{13}C CP (Figure 3c) and ^{2}H→^{13}C CP (Figure 3d). In addition, Figure 3 reveals interesting differences in the two ^{13}C spectra of U−^{2}H,^{13}C,^{15}N-SH3 with 100% ^{1}H back substitution due to the different sources of polarization.

Assembling ^{OC}CP into a New Cross-Polarization Experiment

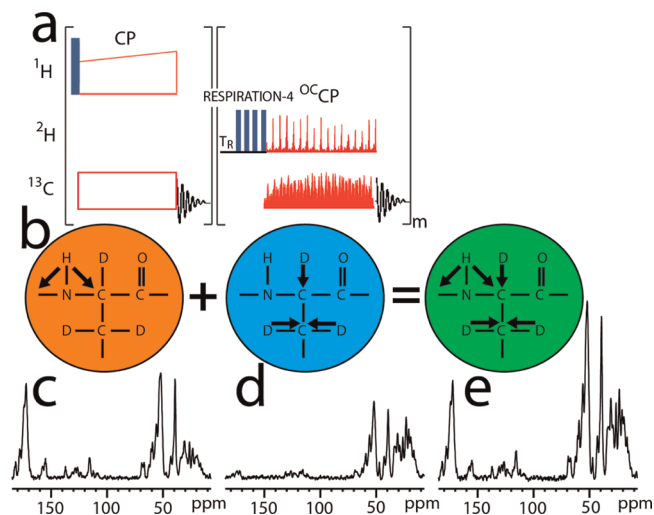Exemplified by the ^{2}H pulse and ^{2}H→^{13}C CP elements, OC proves to be a great tool for pulse sequence design.

FIGURE 3. (a) RAPID ^{1}H→^{13}C/^{2}H→^{13}C CP experiment with the left part representing the ^{1}H-based experiment, interleaved with *m* ^{2}H RESPIRATION-4 ^{OC}CP experiments (right). (b) Cartoons illustrating transfers of magnetization in the two experiments. (c) ^{1}H→^{13}C CP/MAS and (d) ^{2}H→^{13}C RESPIRATION-4 ^{OC}CP spectra extracted from a RAPID ^{1}H→^{13}C/^{2}H→^{13}C CP data set recorded on [100%-U−^{2}H/^{1}H,^{13}C,^{15}N] SH3. (e) Sum of the two spectra in (c) and (d). Figure reproduced from ref 77 with permission.

However, it is evident that most OC sequences are represented by complicated rf waveforms and it may be claimed that they are designed for specific spin systems at given conditions. Both may hamper their widespread application, and may concern the user as being "black-box" elements in experiments otherwise in control of the user through understandable physics. Accordingly, there is an interest in transforming OC sequences into "easier-understandable" sequences resembling those designed by traditional means or at least let OC guide what is possible and subsequently try to reach this analytically.

In favorable cases, insight can be gained by searching for patterns in the OC sequences that may be converted into standard pulse elements. One such example is the Rotor Echo Short Pulse IRradiaTION mediated Cross-Polarization (^{RESPIRATION}CP)[63] sequence which closely resembles the OC sequence for ^{2}H→^{13}C transfer (Figure 2a). The generalized solution (Figure 4a) is a simple rotor synchronized sequence consisting of two "CW periods" with opposite phases on one rf channel followed by simultaneous short pulses on both channels.

The mechanism of ^{RESPIRATION}CP may be described using AHT. The interaction frame effective dipolar Hamiltonian (assuming 90° flip angles for the pulses) for a IS two-spin system is given by

$$\overline{\overline{H}}_{IS}^{D} = \frac{8}{3\pi}(\omega_D^{(1)} + \omega_D^{(-1)})(I_yS_z - I_zS_y) + (\omega_D^{(2)} + \omega_D^{(-2)})(I_yS_y - I_zS_z)$$

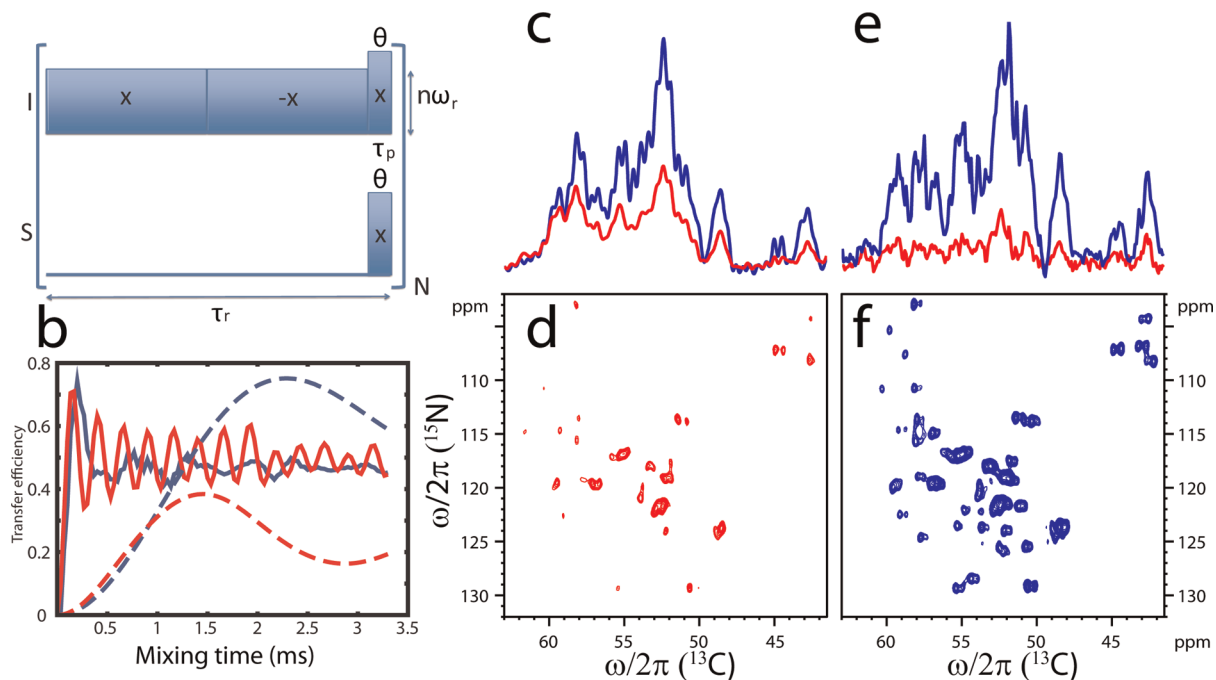revealing recoupling of two pairs of Fourier components. This leads to a transfer efficiency which is higher than the

FIGURE 4. (a) $^{\text{RESPIRATION}}$CP pulse sequence (ω_r, spinning speed; n, small integer; τ_r, rotor period). (b) SIMSPSON[78] simulations comparing $^{\text{RESPIRATION}}$CP (blue) with standard CP (Red) for $^{1}\text{H}\rightarrow^{15}\text{N}$ transfer (solid lines) and $^{15}\text{N}\rightarrow^{13}\text{C}$ transfer (dashed lines). (c) 1D and (d−f) 2D (projections in (e)) NCA spectra of U−^{13}C,^{15}N-GB1 (9.4 T, 30 kHz spinning). Blue spectra are obtained using $^{\text{RESPIRATION}}$CP, while red spectra use conventional ramped CP $^{1}\text{H}\rightarrow^{15}\text{N}$ (350 μs) and adiabatic $^{15}\text{N}\rightarrow^{13}\text{C}$ (3 ms) transfers. Figure reproduced with permission from ref 63. Copyright 2012 American Chemical Society.

celebrated γ_{PR}-encoded sequences,[64] since the terms $\omega^{(1)} + \omega^{(-1)} = b_{\text{IS}} \sin(2\beta_{\text{PR}}) \cos(\gamma_{\text{PR}})/(2\sqrt{2})$ and $\omega^{(2)} + \omega^{(-2)} = -b_{\text{IS}} \sin^2(\beta_{\text{PR}}) \cos(2\gamma_{\text{PR}})/4$ (b_{IS} is the dipolar coupling; constant β_{PR} and γ_{PR} are Euler angles relating rotor and crystal frames of reference, respectively) more efficiently exploit crystallites with different β_{PR} angles.

$^{\text{RESPIRATION}}$CP is not restricted to $^{2}\text{H}\rightarrow^{13}\text{C}$ transfer; it forms a general CP experiment that can be used for a wide range of nuclei and experimental conditions, as exemplified numerically in Figure 4b through improvement of $^{1}\text{H}\rightarrow^{15}\text{N}$ and $^{15}\text{N}\rightarrow^{13}\text{C}$ transfers. Experimental demonstrations are given in Figure 4c−f for U−^{13}C,^{15}N-GB1, where a gain of 30% in sensitivity is observed for the $^{1}\text{H}\rightarrow^{15}\text{N}$ transfer as compared to conventional ramped CP, and a gain of 80% is observed for the $^{15}\text{N}\rightarrow^{13}\text{C}$ transfer relative to conventional adiabatic Double Cross-Polarization (DCP).[65] In combination, this provides a factor of 2 in gain as seen in Figure 4c, which following two consecutive 2D experiments (Figure 4d,f) increased to a factor 4 in gain for the $^{\text{RESPIRATION}}$CP experiment for reasons discussed in the following.

Since $^{\text{RESPIRATION}}$CP only applies CW irradiation on one channel, the overall power requirement is less than that for Hartmann−Hahn matched CP, DCP, and derivative experiments.[57,66−68] Furthermore, $^{\text{RESPIRATION}}$CP is highly tolerant to rf amplitude settings, hereby to a great extent

reducing the cumbersome job of optimizing parameters. On the same token, it reduces sensitivity losses due to rf detuning during long-term experiments for hydrated/lossy samples explaining the additional factor of 2 in gain of sensitivity for the 2D experiments in Figure 4d,f. Another advantage of $^{\text{RESPIRATION}}$CP is its broadbandedness on the channel with CW irradiation. This facilitates recording of NCA and NCO transfers in one experiment, which for conventional/adiabatic DCP requires very strong rf during $^{15}\text{N}-^{13}\text{C}$ recoupling.[69] In another perspective the channel only containing short rf pulses is easily adaptable to nuclei with large anisotropic interactions.

Efficient ^{1}H Decoupling Using CW and rf Pulses

Turning to ^{1}H decoupling in ^{13}C/^{15}N-detected solid-state NMR experiments, many sophisticated techniques exist with improved performance compared to CW decoupling. These includes Two Pulse Phase Modulation (TPPM),[70] Small Phase Incremental Alternation (SPINAL),[71] and broadband versions of these, for example, swept-TPPM,[72] swept-SPINAL,[73] and supercycled-swept-TPPM.[74] These methods have markedly improved the resolution in solid-state NMR spectra, but they have in common that their performance depends critically on careful optimization. This involves the ratio
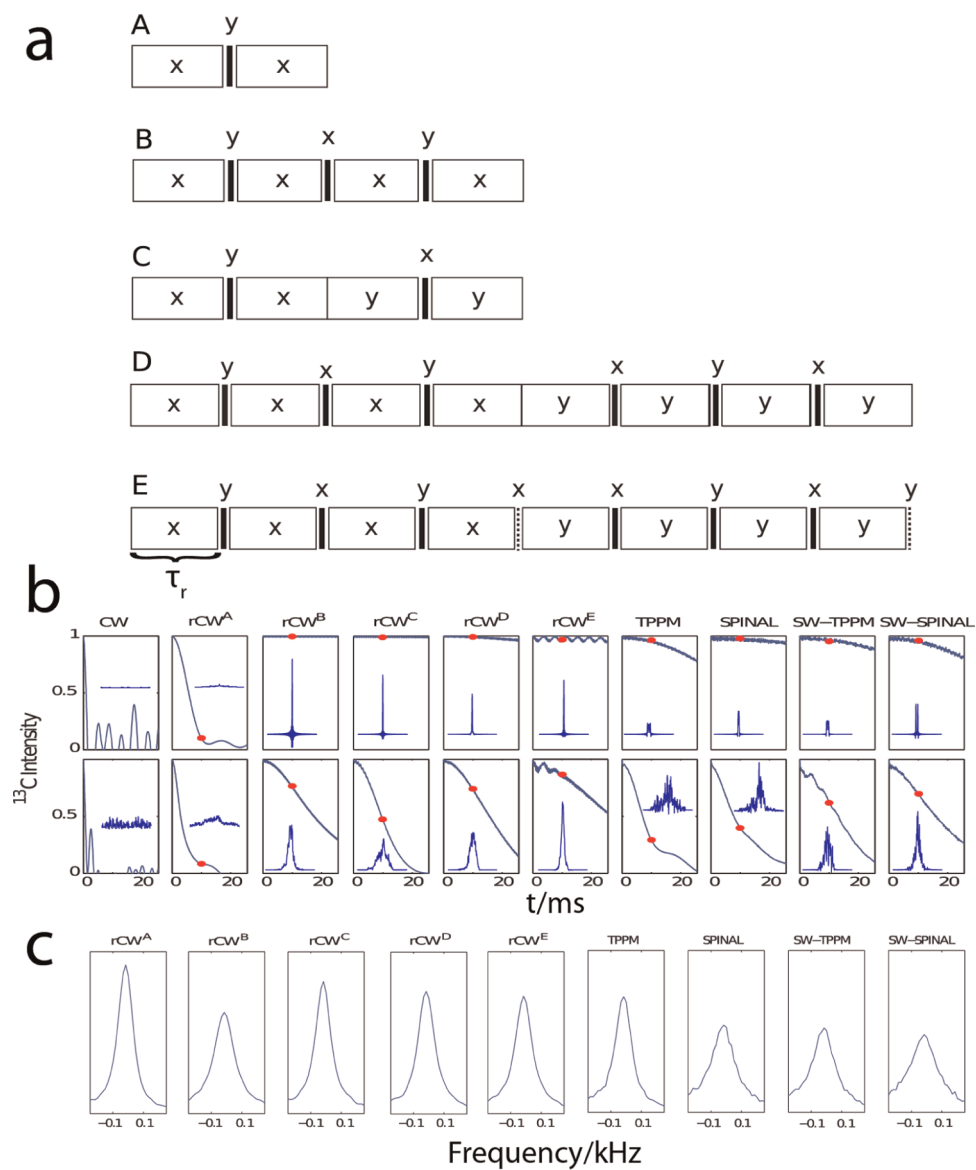
FIGURE 5. (a) rCW decoupling sequences (open boxes, CW irradiation; closed bars, π pulses; dashed bars, $\pi/2$ pulses). (b) Simulations of ^{13}C fids and spectra (± 100 Hz region) using different decoupling sequences for CH (top) and CH$_2$ (bottom; spectra scaled by factor 10). Average decoupling rf-field strengths of 93.7 kHz (for rCW: 90 kHz CW and 222 kHz pulses), 20 kHz spinning, and a static field of 850 MHz. Red dots indicate 10 ms intensity. (c) Experimental comparison of ^{13}C spectra (850 MHz spectrometer, 20 kHz spinning, 30 ms acquisition, no apodization) for 25% ^{13}C-glycine using 70 kHz rf decoupling field strength with 222 kHz refocusing pulses. Figure reproduced from ref 75 with permission.

between the rf field strength and the spinning speed, but also pulse length and phase parameters.

To remedy these problems and make decoupling robust toward anisotropic shielding at high fields, we undertook development of efficient decoupling sequences based on AHT analysis of a simple ^{13}C–^{1}H (in the following denoted S and I, respectively) spin system.[75] This exposed a critical second-order term proportional to $2I_xS_z$ and two-third-order terms proportional to $2I_zS_z$ and $2I_yS_z$, appearing as cross terms between dipolar coupling and chemical shielding anisotropy of the I spin. By incorporation of a *y*-phase

π-pulse, it is possible to refocus evolution due to the second-order and $2I_zS_z$ third-order terms. Further incorporation of an *x*-phase π-pulse refocuses evolution due to the $2I_yS_z$ term. This approach yields the decoupling sequences *A* and *B* in Figure 5a. Another attempt to remove second- and third-order terms uses phase-alternated elements. In the analysis semicontinuous BCH[40] calculations are applied, and the resulting sequences are shown as variants *C* and *D* in Figure 5a. Introduction of $\pi/2$-purging pulses downscale terms unaffected by π-pulses, for example, terms like $4I_{1x}I_{2x}S_z$ which occur if two or more coupled protons

are present, leading to sequence *E* in Figure 5a. Common to the sequences *A*−*E* is the refocusing element, and they are named rCW[A]-rCW[E] (rCW: refocused CW).

The rCW schemes are compared to CW and state-of-the-art decoupling through numerical simulations in Figure 5b assuming CH (top) and CH_2 (bottom) spin systems. Both fids and spectra are shown, and the red dots indicate intensities in the fids at 10 ms. It is evident that rCW has a great potential for heteronuclear decoupling for CH and CH_2 spin systems, in the latter case also handling homonuclear couplings with a visible effect of the purging pulses in the rCW[E] sequence. The performance is analyzed experimentally in Figure 5c, through line shapes observed for C[α] in glycine in the case of decoupling with rf field strengths in the order of 70 kHz. Optimum conditions are found for moderate CW rf-field strengths combined with high-power refocusing pulses, under which conditions rCW outperform the state-of-the-art sequences. The somewhat peculiar result that the rCW[A] sequence is found most efficient is ascribed mainly to a small third-order $2I_yS_z$ term for the glycine sample. Overall, the performance of the rCW sequences are at least on par with the state-of-the-art sequences with the additional gain of easier optimizization. Furthermore, the rCW sequences are found to be well-performing for large chemical shift anisotropies as evidenced in a recent study of ^{19}F decoupling.[76]

We have in this Account demonstrated how biological solid-state NMR may be improved in terms of *sensitivity* and *resolution* through systematic design of rf pulses, recoupling, sampling, and decoupling methods. Our design involved optimal control and average Hamiltonian analysis, hereby serving to demonstrate that combinations of these tools may lead to efficient, yet analytically understandable pulse sequences with impact on experimental performance.

BIOGRAPHICAL INFORMATION

Morten Bjerring received his Ph.D. from Aarhus University in 2005 and has since been manager of the NMR laboratories in the Center of Insoluble Protein Structures (inSPIN). He has published 26 papers.

Sheetal Jain finished his M.Sc. from Indian Institute of Science Education and Research (IISER), Pune, India. Currently, he is pursuing his Ph.D. from iNANO at Aarhus University. He has published two papers.

Berit Paaske received her M.Sc. from Aarhus University in 2009 and is now finishing her Ph.D. at the same place. She has published three papers.

Joachim M. Vinther reveived his M.Sc. from the University of Copenhagen in 2009 and has just finished his Ph.D. from Aarhus University. He has published three papers.

Niels Chr. Nielsen received his Ph.D. from Aarhus University in 1989. He established the Laboratory for Biomolecular NMR at Aarhus University as part of the Danish Biotechnological Instrument Center. In 2005, he established the Center of Insoluble Protein Structures (inSPIN) supported by the Danish National Research Foundation. He was one of the founders and now Director of the Interdisciplinary Nanoscience Center (iNANO) at Aarhus University. He has published 217 papers within development and application of NMR and MRI in nanoscience and structural biology.

FOOTNOTES

REFERENCES

1 Andrew, E. R.; Bradbury, A.; Eades, R. G. Removal of Dipolar Broadening of Nuclear Magnetic Resonance Spectra of Solids by Specimen Rotation. *Nature* **1959**, *183*, 1802–1803.

2 Lemaster, D. M. Deuteration in Protein Proton Magnetic-Resonance. *Methods Enzym.* **1989**, *177*, 23–43.

3 Kay, L. E.; Gardner, K. H. Solution NMR spectroscopy beyond 25 kDa. *Curr. Opin. Struct. Biol.* **1997**, *7*, 722–731.

4 Castellani, F.; van Rossum, B.; Diehl, A.; Schubert, M.; Rehbein, K.; Oschkinat, H. Structure of a protein determined by solid-state magic-angle-spinning NMR spectroscopy. *Nature* **2002**, *420*, 98–102.

5 Lundstrom, P.; Teilum, K.; Carstensen, T.; Bezsonova, I.; Wiesner, S.; Hansen, D. F.; Religa, T. L.; Akke, M.; Kay, L. E. Fractional C-13 enrichment of isolated carbons using 1-C-13 - or 2-C-13 -glucose facilitates the accurate measurement of dynamics at backbone C-alpha and side-chain methyl positions in proteins. *J. Biomol. NMR* **2007**, *38*, 199–212.

6 Renault, M.; Tommassen-van Boxtel, R.; Bos, M. P.; Post, J. A.; Tommassen, J.; Baldus, M. Cellular solid-state nuclear magnetic resonance spectroscopy. *Proc. Natl. Acad. Sci. U.S.A.* **2012**, *109*, 4863–4868.

7 Kulminskaya, N. V.; Pedersen, M. O.; Bjerring, M.; Underhaug, J.; Miller, M.; Frigaard, N. U.; Nielsen, J. T.; Nielsen, N. C. In Situ Solid-State NMR Spectroscopy of Protein in Heterogeneous Membranes: The Baseplate Antenna Complex of Chlorobaculum tepidum. *Angew. Chem., Int. Ed.* **2012**, *51*, 6891–6895.

8 Opella, S. J. NMR and membrane proteins. *Nat. Struct. Biol.* **1997**, *4*, 845–848.

9 Opella, S. J.; Marassi, F. M.; Gesell, J. J.; Valente, A. P.; Kim, Y.; Oblatt-Montal, M.; Montal, M. Structures of the M2 channel-lining segments from nicotinic acetylcholine and NMDA receptors by NMR spectroscopy. *Nat. Struct. Biol.* **1999**, *6*, 374–379.

10 De Angelis, A. A.; Howell, S. C.; Nevzorov, A. A.; Opella, S. J. Structure determination of a membrane protein with two trans-membrane helices in aligned phospholipid bicelles by solid-state NMR spectroscopy. *J. Am. Chem. Soc.* **2006**, *128*, 12256–12267.

11 Marassi, F. M.; Opella, S. J. Simultaneous assignment and structure determination of a membrane protein from NMR orientational restraints. *Protein Sci.* **2003**, *12*, 403–411.

12 Yao, Y.; Barghava, N.; Kim, J.; Niedenueis, M.; Marassi, F. M. Molecular Structure and Peptidoglycan Recognition of Mycobacterium tuberculosis ArfA (Rv0899). *J. Mol. Biol.* **2012**, *416*, 208–220.

13 Vosegaard, T.; Kamihira-Ishijima, M.; Watts, A.; Nielsen, N. C. Helix conformations in 7TM membrane proteins determined using oriented-sample solid-state NMR with multiple residue-specific N-15 labeling. *Biophys. J.* **2008**, *94*, 241–250.

14 Marassi, F. M.; Das, B. B.; Lu, G. J.; Nothnagel, H. J.; Park, S. H.; Son, W. S.; Tian, Y.; Opella, S. J. Structure determination of membrane proteins in five easy pieces. *Nat. Methods* **2011**, *55*, 363–369.

15 Manolikas, T.; Herrmann, T.; Meier, B. H. Protein structure determination from C-13 spin-diffusion solid-state NMR spectroscopy. *J. Am. Chem. Soc.* **2008**, *130*, 3959–3966.

16 Zech, S. G.; Wand, A. J.; McDermott, A. E. Protein structure determination by high-resolution solid-state NMR spectroscopy: Application to microcrystalline ubiquitin. *J. Am. Chem. Soc.* **2005**, *127*, 8618–8626.

17 Franks, W. T.; Wylie, B. J.; Schmidt, H. L. F.; Nieuwkoop, A. J.; Mayrhofer, R. M.; Shah, G. J.; Graesser, D. T.; Rienstra, C. M. Dipole tensor-based atomic-resolution structure determination of a nanocrystalline protein by solid-state NMR. *Proc. Natl. Acad. Sci. U.S.A.* **2008**, *105*, 4621–4626.

18 Loquet, A.; Bardiaux, B.; Gardiennet, C.; Blanchet, C.; Baldus, M.; Nilges, M.; Malliavin, T.; Boeckmann, A. 3D structure determination of the Crh protein from highly ambiguous solid-state NMR restraints. *J. Am. Chem. Soc.* **2008**, *130*, 3579–3589.

19 Bertini, I.; Bhaumik, A.; De Paepe, G.; Griffin, R. G.; Lelli, M.; Lewandowski, J. R.; Luchinat, C. High-Resolution Solid-State NMR Structure of a 17.6 kDa Protein. *J. Am. Chem. Soc.* **2010**, *132*, 1032–1040.

20 Jaroniec, C. P.; MacPhee, C. E.; Bajaj, V. S.; McMahon, M. T.; Dobson, C. M.; Griffin, R. G. High-resolution molecular structure of a peptide in an amyloid fibril determined by magic angle spinning NMR spectroscopy. *Proc. Natl. Acad. Sci. U.S.A.* **2004**, *101*, 711–716.

21 Iwata, K.; Fujiwara, T.; Matsuki, Y.; Akutsu, H.; Takahashi, S.; Naiki, H.; Goto, Y. 3D structure of amyloid protofilaments of beta(2)-microglobulin fragment probed by solid-state NMR. *Proc. Natl. Acad. Sci. U.S.A.* **2006**, *103*, 18119–18124.

22 Wasmer, C.; Lange, A.; Van Melckebeke, H.; Siemer, A. B.; Riek, R.; Meier, B. H. Amyloid fibrils of the HET-s(218−289) prion form a beta solenoid with a triangular hydrophobic core. *Science* **2008**, *319*, 1523–1526.

23 Bertini, I.; Gonnelli, L.; Luchinat, C.; Mao, J.; Nesi, A. A New Structural Model of A beta(40) Fibrils. *J. Am. Chem. Soc.* **2011**, *133*, 16013–16022.

24 Nielsen, J. T.; Bjerring, M.; Jeppesen, M. D.; Pedersen, R. O.; Pedersen, J. M.; Hein, K. L.; Vosegaard, T.; Skrydstrup, T.; Otzen, D. E.; Nielsen, N. C. Unique Identification of Supramolecular Structures in Amyloid Fibrils by Solid-State NMR Spectroscopy. *Angew. Chem., Int. Ed.* **2009**, *48*, 2118–2121.

25 Cady, S. D.; Schmidt-Rohr, K.; Wang, J.; Soto, C. S.; DeGrado, W. F.; Hong, M. Structure of the amantadine binding site of influenza M2 proton channels in lipid bilayers. *Nature* **2010**, *463*, 689–693.

26 Lange, A.; Giller, K.; Hornig, S.; Martin-Eauclaire, M. F.; Pongs, O.; Becker, S.; Baldus, M. Toxin-induced conformational changes in a potassium channel revealed by solid-state NMR. *Nature* **2006**, *440*, 959–962.

27 Sivertsen, A. C.; Bayro, M. J.; Belenky, M.; Griffin, R. G.; Herzfeld, J. Solid-State NMR Characterization of Gas Vesicle Structure. *Biophys. J.* **2010**, *99*, 1932–1939.

28 Loquet, A.; Sgourakis, N. G.; Gupta, R.; Giller, K.; Riedel, D.; Goosmann, C.; Griesinger, C.; Kolbe, M.; Baker, D.; Becker, S.; Lange, A. Atomic model of the type III secretion system needle. *Nature* **2012**, *486*, 276–279.

29 Jehle, S.; Rajagopal, P.; Bardiaux, B.; Markovic, S.; Kuhne, R.; Stout, J. R.; Higman, V. A.; Klevit, R. E.; van Rossum, B. J.; Oschkinat, H. Solid-state NMR and SAXS studies provide a structural basis for the activation of alpha B-Crystallin oligomers. *Nat. Struct. Mol. Biol.* **2010**, *17*, 1037–1042.

30 Mcdermott, A. E.; Creuzet, F. J.; Kolbert, A. C.; Griffin, R. G. High-Resolution Magic-Angle-Spinning Nmr-Spectra of Protons in Deuterated Solids. *J. Magn. Reson.* **1992**, *98*, 408–413.

31 Reif, B.; Griffin, R. G. 1H detected 1H,15N correlation spectroscopy in rotating solids. *J. Magn. Reson.* **2003**, *160*, 78–83.

32 Agarwal, V.; Diehl, A.; Skrynnikov, N.; Reif, B. High resolution H-1 detected H-1,C-13 correlation spectra in MAS solid-state NMR using deuterated proteins with selective H-1,H-2 isotopic labeling of methyl groups. *J. Am. Chem. Soc.* **2006**, *128*, 12620–12621.

33 Chevelkov, V.; Rehbein, K.; Diehl, A.; Reif, B. Ultrahigh resolution in proton solid-state NMR spectroscopy at high levels of deuteration. *Angew. Chem., Int. Ed.* **2006**, *45*, 3878–3881.

34 Linser, R.; Dasari, M.; Hiller, M.; Higman, V.; Fink, U.; Lopez Del Amo, J. M.; Markovic, S.; Handel, L.; Kessler, B.; Schmieder, P.; Oesterhelt, D.; Oschkinat, H.; Reif, B. Proton-detected solid-state NMR spectroscopy of fibrillar and membrane proteins. *Angew. Chem., Int. Ed.* **2011**, *50*, 4508–4512.

35 Lalli, D.; Schanda, P.; Chowdhury, A.; Retel, J.; Hiller, M.; Higman, V. A.; Handel, L.; Agarwal, V.; Reif, B.; van Rossum, B.; Akbey, U.; Oschkinat, H. Three-dimensional deuterium-carbon correlation experiments for high-resolution solid-state MAS NMR spectroscopy of large proteins. *J. Biomol. NMR* **2011**, *51*, 477–485.

36 Akbey, U.; Lange, S.; Franks, W. T.; Linser, R.; Rehbein, K.; Diehl, A.; van Rossum, B. J.; Reif, B.; Oschkinat, H. Optimum levels of exchangeable protons in perdeuterated proteins for proton detection in MAS solid-state NMR spectroscopy. *J. Biomol. NMR* **2010**, *46*, 67–73.

37 Asami, S.; Szekely, K.; Schanda, P.; Meier, B. H.; Reif, B. Optimal degree of protonation for H-1 detection of aliphatic sites in randomly deuterated proteins as a function of the MAS frequency. *J. Biomol. NMR* **2012**, *54*, 155–168.

38 Hologne, M.; Faelber, K.; Diehl, A.; Reif, B. Characterization of dynamics of perdeuterated proteins by MAS solid-state NMR. *J. Am. Chem. Soc.* **2005**, *127*, 11208–11209.

39 Haeberlen, U.; Waugh, J. S. Coherent Averaging Effects in Magnetic Resonance. *Phys. Rev.* **1968**, *175*, 453–&.

40 Hohwy, M.; Nielsen, N. C. Systematic design and evaluation of multiple-pulse experiments in nuclear magnetic resonance spectroscopy using a semi-continuous Baker-Campbell-Hausdorff expansion. *J. Chem. Phys.* **1998**, *109*, 3780–3791.

41 Untidt, T. S.; Nielsen, N. C. Closed solution to the Baker-Campbell-Hausdorff problem: Exact effective Hamiltonian theory for analysis of nuclear-magnetic-resonance experiments. *Phys. Rev. E* **2002**, *65*, 021108.

42 Schmidt, A.; Vega, S. The Floquet Theory of Nuclear-Magnetic-Resonance Spectroscopy of Single Spins and Dipolar Coupled Spin Pairs in Rotating Solids. *J. Chem. Phys.* **1992**, *96*, 2655–2680.

43 Pontryagin, L. S. *The mathematical theory of optimal processes*; Interscience Publishers: New York, 1962.

44 Khaneja, N.; Reiss, T.; Kehlet, C.; Schulte-Herbruggen, T.; Glaser, S. J. Optimal control of coupled spin dynamics: design of NMR pulse sequences by gradient ascent algorithms. *J. Magn. Reson.* **2005**, *172*, 296–305.

45 Tosner, Z.; Vosegaard, T.; Kehlet, C.; Khaneja, N.; Glaser, S. J.; Nielsen, N. C. Optimal control in NMR spectroscopy: Numerical implementation in SIMPSON. *J. Magn. Reson.* **2009**, *197*, 120–134.

46 Maximov, I. I.; Tosner, Z.; Nielsen, N. C. Optimal control design of NMR and dynamic nuclear polarization experiments using monotonically convergent algorithms. *J. Chem. Phys.* **2008**, *128*, 184505.

47 Maximov, I. I.; Salomon, J.; Turinici, G.; Nielsen, N. C. A smoothing monotonic convergent optimal control algorithm for nuclear magnetic resonance pulse sequence design. *J. Chem. Phys.* **2010**, *132*, 084107.

48 Vinding, M. S.; Maximov, I. I.; Tosner, Z.; Nielsen, N. C. Fast numerical design of spatial-selective rf pulses in MRI using Krotov and quasi-Newton based optimal control methods. *J. Chem. Phys.* **2012**, *137*, 054203.

49 Reiss, T. O.; Khaneja, N.; Glaser, S. J. Time-optimal coherence-order-selective transfer of in-phase coherence in heteronuclear IS spin systems. *J. Magn. Reson.* **2002**, *154*, 192–195.

50 Kehlet, C. T.; Sivertsen, A. C.; Bjerring, M.; Reiss, T. O.; Khaneja, N.; Glaser, S. J.; Nielsen, N. C. Improving solid-state NMR dipolar recoupling by optimal control. *J. Am. Chem. Soc.* **2004**, *126*, 10202–10203.

51 Kehlet, C.; Bjerring, M.; Sivertsen, A. C.; Kristensen, T.; Enghild, J. J.; Glaser, S. J.; Khaneja, N.; Nielsen, N. C. Optimal control based NCO and NCA experiments for spectral assignment in biological solid-state NMR spectroscopy. *J. Magn. Reson.* **2007**, *188*, 216–230.

52 Xu, D.; King, K. F.; Zhu, Y.; McKinnon, G. C.; Liang, Z. P. Designing multichannel, multidimensional, arbitrary flip angle RF pulses using an optimal control approach. *Magn. Reson. Med.* **2008**, *59*, 547–560.

53 Li, J. S.; Ruths, J.; Yu, T. Y.; Arthanari, H.; Wagner, G. Optimal pulse design in quantum control: A unified computational method. *Proc. Natl. Acad. Sci. U.S.A.* **2011**, *108*, 1879–1884.

54 Wei, D.; Akbey, U.; Paaske, B.; Oschkinat, H.; Reif, B.; Bjerring, M.; Nielsen, N. C. Optimal 2H Rf Pulses and 2H-13C Cross-Polarization Methods for Solid-State 2H MAS NMR of Perdeuterated Proteins. *J. Phys. Chem. Lett.* **2011**, *2*, 1289–1294.

55 Vitzthum, V.; Caporini, M. A.; Ulzega, S.; Bodenhausen, G. Broadband excitation and indirect detection of nitrogen-14 in rotating solids using Delays Alternating with Nutation (DANTE). *J. Magn. Reson.* **2011**, *212*, 234–239.

56 Pines, A.; Waugh, J. S.; Gibby, M. G. Proton-Enhanced Nuclear Induction Spectroscopy - Method for High-Resolution Nmr of Dilute Spins in Solids. *J. Chem. Phys.* **1972**, *56*, 1776–1777.

57 Metz, G.; Wu, X. L.; Smith, S. O. Ramped-Amplitude Cross-Polarization in Magic-Angle-Spinning Nmr. *J. Magn. Reson., Ser A* **1994**, *110*, 219–227.

58 Wickramasinghe, N. P.; Shaibat, M.; Ishii, Y. Enhanced sensitivity and resolution in H-1 solid-state NMR spectroscopy of paramagnetic complexes under very fast magic angle spinning. *J. Am. Chem. Soc.* **2005**, *127*, 5796–5797.

59 Wickramasinghe, N. P.; Kotecha, M.; Samoson, A.; Past, J.; Ishii, Y. Sensitivity enhancement in C-13 solid-state NMR of protein microcrystals by use of paramagnetic metal ions for optimizing H-1 T-1 relaxation. *J. Magn. Reson.* **2007**, *184*, 350–356.

60 Linser, R.; Chevelkov, V.; Diehl, A.; Reif, B. Sensitivity enhancement using paramagnetic relaxation in MAS solid-state NMR of perdeuterated proteins. *J. Magn. Reson.* **2007**, *189*, 209–216.

61 Wickramasinghe, N. P.; Parthasarathy, S.; Jones, C. R.; Bhardwaj, C.; Long, F.; Kotecha, M.; Mehboob, S.; Fung, L. W. M.; Past, J.; Samoson, A.; Ishii, Y. Nanomole-scale protein solid-state NMR by breaking intrinsic H-1 T-1 boundaries. *Nat. Methods* **2009**, *6*, 215–218.

62 Lopez, J. J.; Kaiser, C.; Asami, S.; Glaubitz, C. Higher Sensitivity through Selective C-13 Excitation in Solid-State NMR Spectroscopy. *J. Am. Chem. Soc.* **2009**, *131*, 15970–15971.

63 Jain, S.; Bjerring, M.; Nielsen, N. C. Efficient and Robust Heteronuclear Cross-Polarization for High-Speed-Spinning Biological Solid-State NMR Spectroscopy. *J. Phys. Chem. Lett.* **2012**, *3*, 703–708.

64 Nielsen, N. C.; Bildsoe, H.; Jakobsen, H. J.; Levitt, M. H. Double-Quantum Homonuclear Rotary Resonance - Efficient Dipolar Recovery in Magic-Angle-Spinning Nuclear-Magnetic-Resonance. *J. Chem. Phys.* **1994**, *101*, 1805–1812.

65 Schaefer, J.; McKay, R. A.; Stejskal, E. O Double-cross-polarization NMR of solids. *J. Magn. Reson.* **1979**, *34*, 443–447.

66 Baldus, M.; Geurts, D. G.; Hediger, S.; Meier, B. H. Efficient N-15-C-13 polarization transfer by adiabatic-passage Hartmann-Hahn cross polarization. *J. Magn. Reson., Ser A* **1996**, *118*, 140–144.

67 Raya, J.; Hirschinger, J. Application of rotor-synchronized amplitude-modulated cross-polarization in a C-13-H-1 spin pair under fast magic-angle spinning. *J. Magn. Reson.* **1998**, *133*, 341–351.

68 Hu, B.; Amoureux, J. P.; Trebosc, J.; Hafner, S. Through-space MP-CPMAS experiments between spin-1/2 and half-integer quadrupolar nuclei in solid-state NMR. *J. Magn. Reson.* **2008**, *192*, 8–16.

69 Bjerring, M.; Nielsen, A. B.; Tosner, Z.; Nielsen, N. C. Broadband heteronuclear dipolar recoupling without H-1 decoupling in solid-state NMR using simple cross-polarization methods. *Chem. Phys. Lett.* **2010**, *494*, 326–330.

70 Bennett, A. E.; Rienstra, C. M.; Auger, M.; Lakshmi, K. V.; Griffin, R. G. Heteronuclear Decoupling in Rotating Solids. *J. Chem. Phys.* **1995**, *103*, 6951–6958.

71 Fung, B. M.; Khitrin, A. K.; Ermolaev, K. An Improved Broadband Decoupling Sequence for Liquid Crystals and Solids. *J. Magn. Reson.* **2000**, *142*, 97–101.

72 Thakur, R. S.; Kurur, N. D.; Madhu, P. K. Swept-frequency two-pulse phase modulation for heteronuclear dipolar decoupling in solid-state NMR. *Chem. Phys. Lett.* **2006**, *426*, 459–463.

73 Chandran, C. V.; Brauniger, T. Efficient heteronuclear dipolar decoupling in solid-state NMR using frequency-swept SPINAL sequences. *J. Magn. Reson.* **2009**, *200*, 226–232.

74 Augustine, C.; Kurur, N. D. Supercycled SWf-TPPM sequence for heteronuclear dipolar decoupling in solid-state nuclear magnetic resonance. *J. Magn. Reson.* **2011**, *209*, 156–160.

75 Vinther, J. M.; Nielsen, A. B.; Bjerring, M.; van Eck, E. R. H.; Kentgens, A. P. M.; Khaneja, N.; Nielsen, N. C. Refocused continuous-wave decoupling: A new approach to heteronuclear dipolar decoupling in solid-state NMR spectroscopy. *J. Chem. Phys.* **2012**, *137*, 214202.

76 Vinther, J. M.; Khaneja, N.; Nielsen, N. C. Robust and efficient 19F heteronuclear dipolar decoupling using refocused continuous-wave rf irradiation. *J. Magn. Reson.* **2013**, *226*, 88–92.

77 Bjerring, M.; Paaske, B.; Oschkinat, H.; Akbey, U.; Nielsen, N. C. Rapid solid-state NMR of deuterated proteins by interleaved cross-polarization from H-1 and H-2 nuclei. *J. Magn. Reson.* **2012**, *214*, 324–328.

78 Bak, M.; Rasmussen, J. T.; Nielsen, N. C. SIMPSON: A general simulation program for solid-state NMR spectroscopy. *J. Magn. Reson.* **2000**, *147*, 296–330.